Theor Appl Climatol (2013) 112:89–98
DOI 10.1007/s00704-012-0717-8

ORIGINAL PAPER

The surface urban heat island in the city of Brno (Czech Republic) derived from land surface temperatures and selected reasons for its spatial variability

Petr Dobrovolný

Received: 9 December 2011 / Accepted: 5 July 2012 / Published online: 20 July 2012

Abstract Thermal infrared images from Landsat satellites are used to derive land surface temperatures (LST) and to calculate the intensity of the surface urban heat island (UHI) during the summer season in and around the city of Brno (Czech Republic). Overall relief, land use structure, and the distribution of built-up areas determine LST and UHI spatial variability in the study area. Land-cover classes, amount and vigor of vegetation, and density of built-up areas are used as explanatory variables. The highest LST values typically occur in industrial and commercial areas, which contribute significantly to surface UHI intensity. The intensity of surface UHI, defined as the difference between mean LST for urban and rural areas, reached 4.2 and 6.7 °C in the two images analyzed. Analysis of two surface characteristics in terms of the amount of vegetation cover, represented by normalized difference vegetation index, demonstrates the predominance of LST variability (56–67 % of explained variance) over the degree of urbanization as represented by density of buildings (37–40 % of LST variance).

1 Introduction

Urban populations are increasing, and with them vulnerability to weather extremes and adverse climate conditions, with all the concomitant threats to human life and material well-being. Currently, around 50 % of the world population lives in large cities, in the developed countries as many as 75 % (Lambin and Geist 2006). Changes in the character of the active surface brought about by buildings, air contamination, and production of waste heat are the main factors that contribute to the creation of the specific climate of urban areas. Built-up areas considered as a type of active surface, together with human activities within cities, form a hierarchical system, from the micro level of individual buildings to the regional level. According to Grimmond (2006), an urban climate can also be studied at several different degrees of resolution.

The most typical manifestation of urban climate is the urban heat island (UHI), a term that encapsulates the higher temperatures that occur in built-up areas compared to natural landscapes in their surroundings. UHI is also the feature most analyzed in urban climatology (Stewart 2011) and, as mentioned by Oke (1997) or more recently in a review collated by Arnfiled (2003), many types of UHI may be defined, depending on differences in processes of energy exchange, variations in scale, or methods employed in data acquisition. Atmospheric UHI is usually studied largely by means of air temperature measurements; its intensity can generally be expressed as the difference between stations located in urban and rural environments. Temporal variability of UHI is particularly accessible to such an approach, in great detail.

Surface UHI can also be measured and mapped. This is a matter of urban–rural differences in land surface temperatures (LST) and remote sensing offers several very effective ways to study it (Voogt and Oke 2003). Because a

P. Dobrovolný (✉)
Department of Geography, Masaryk University,
Kotlářská 2,
611-37 Brno, Czech Republic
e-mail: dobro@sci.muni.cz

considerable spatial variability of temperature regime is also typical of an urban environment, thermal infrared imagery provides valuable information not only about the intensity of surface UHI, but also consistent information about spatial variability of surface temperatures within urbanized areas (Weng 2009).

In the course of the last two decades, thermal infrared imagery from several satellite systems, at various spatial and spectral resolutions, has been employed in the analysis of LST and surface UHI for different cities. Thus, e.g., Dousset et al. (2011) used NOAA data for characterizing the spatial features of a heat-wave in the region of Paris, France, in summer 2003. Surface temperatures derived from MODIS data were utilized for UHI analysis for several Hungarian cities by Pongracz et al. (2006) and for Bucharest, Romania (Cheval and Dumitrescu 2009). Tomlinson et al. (2010) used MODIS data to characterize summer surface UHI in Birmingham, England.

Studies based on spatially well-resolved data from the Landsat and Terra (ASTER) satellites (Qin et al. 2001; Li et al. 2004; Sobrino et al. 2004) have confirmed that LSTs in urban areas vary widely with location and that surface UHI very frequently exhibits spatial patterns that are related to differences in the surface parameters of the urban environment, such as type and density of built-up areas and occurrence of vegetation. As Arnfield (2003) aptly notes, many urban remote sensing studies confirm that "UHIs are more diverse than originally suspected".

Many recent studies of LST variability and surface UHI intensity have focused on large metropolitan areas such as Athens (Stathopoulou and Cartalis 2007), Paris, and Los Angeles (Dousset et al. 2011). Some studies analyzed these features in climatic zones different from the central European, especially for cities with rapid urbanization (Nichol 1998; Kato and Yasushi 2005; Hu and Jia 2010; Tan et al. 2010).

The main objective of the current paper is, by means of thermal infrared satellite imagery and GIS resources, to assess the causes of spatial variability in the thermal environment of the city of Brno, in the Czech Republic (CR), as an example of a medium-sized central European city located in complex terrain. Further, LST fields derived from thermal imagery and land use categories are used for analysis of surface UHI intensity. Finally, two different surface parameters are used as predictors for explanation of LST spatial distribution in a regression model. The study area and data used are described in Section 2. In the third section, we provide basic information on methodology. Section 4 summarizes the main results and finally we compare our findings with similar studies and discuss future prospects.

2 Study area and data employed

The study area is situated in the southeastern part of the Czech Republic (Fig. 1). Brno (49.2 N, 16.5 E) is the second largest city in the CR (population 400,000; cadastral area 230 km^2) and is characterized by a basin position with a complex terrain. Altitudes range from 190 to 479 m, with the higher elevations lying largely in the western and northern parts of the region, while lower and flatter terrain is typical of the southern and eastern parts. There is a water reservoir (area ~2.6 km^2) located on the northwest border of the built-up area. The study area lies in one of the warmest and the driest regions in the CR. Mean annual temperature reaches 9.4 °C while mean annual precipitation is about 500 mm (1961–2000 reference period).

The city's location at the confluence of two rivers and a complex relief predispose to a characteristic spatial distribution of land-cover categories. A high density of built-up areas occurs in the historical city center, largely residential (20 % of the study area), but especially in the industrial zones and large shopping centers with high percentages of impervious surfaces (area almost 14 %). Several large parks are located relatively close to the city center. Further from the center, individual land-cover categories form a mosaic of different surface types, such as blocks of flats, gardens, allotments, and agricultural fields. Arable land and grasslands cover 34 % of the study region and are situated mostly in the south, while forests take up 29 % of the region and are mostly to be found west and north of the built-up area, at higher elevations.

LST fields were constructed from available Landsat thermal infrared imagery. The first scene was acquired with Landsat Enhanced Thematic Mapper Plus (ETM+) on May 24, 2001 at 9:35 GMT. Thermal band 6.1 of ETM+ (10.4–12.5 μm) has a ground resolution of 60 m. The second batch of thermal imagery came from Landsat 5 Thematic Mapper (TM), which has a lower ground resolution (120 m). This image was acquired on June 15, 2006 at the same time. On both dates, typical anticyclone-type weather prevailed, with no clouds, sky clear and calm. However, the air temperatures on the first date (mean air temperature, 17.6 °C; minimum, 8.4 °C; maximum, 23.3 °C) were significantly lower compared with the second date (mean air temperature, 20.6 °C; minimum, 10.6 °C; maximum, 25.9 °C).

Several GIS resources other than thermal imagery were employed. The land-use map was compiled from satellite data by means of an object-oriented image analysis and supervised classification approach. The original map comprised 17 classes. These classes, however, represented land utilization rather than land-cover

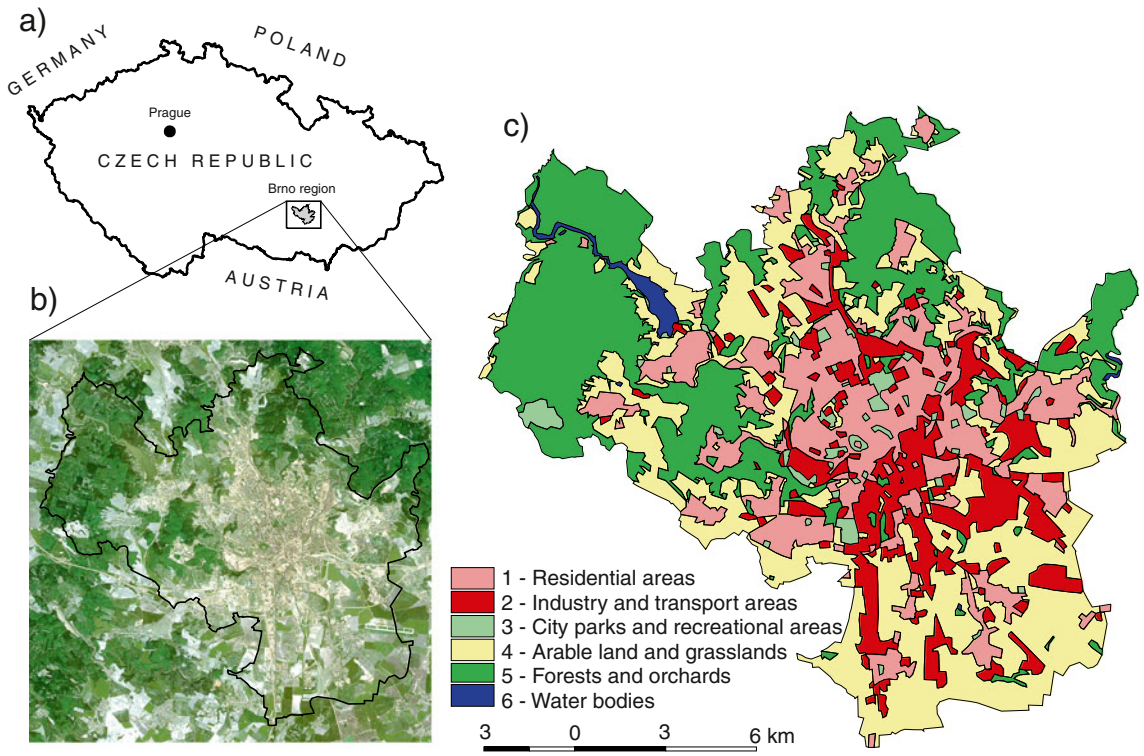

Fig. 1 Location of the study area within the Czech Republic (**a**), character of the land-cover (**b**), land-cover map (**c**)

and some classes did not show significant differences in surface-leaving radiance. For example, the category of grasslands within city neighborhoods has the same surface cover and the same emissive characteristics as the category of parks. Because these two classes were the same in terms of land-cover, they were combined into a single category. Moreover, the areal extent of certain original land-use categories (sports grounds and mining sites, for example) proved too small for the spatial resolution of thermal imagery (60 and 120 m, respectively). Largely for these reasons, certain classes were combined and a land-cover map with six categories (as presented in Fig. 1c) was used to quantify the influence of individual categories on spatial variability in LST and surface UHI spatial structure. The study area was further interpreted in terms of GIS vector database building blocks, which served to construct a measure of density of buildings as a further predictor explaining LST spatial variability and surface UHI spatial patterns (see Section 3).

3 Methods

Thermal satellite imagery measures surface leaving radiance modified by the atmosphere and LST retrieval from thermal infrared imagery is generally calculated by reversing Planck's law (which is, however, exactly valid for only black-body objects). Atmospheric and emissivity corrections are required in order to apply this function to real surfaces. There exist several methods of thermal remote sensing for urban climate applications. These approaches differ in particular in the number of thermal bands available (Qin et al. 2001; Dash et al. 2002; Weng 2009; Hu and Jia 2010). Since Landsat satellites provide only a single thermal infrared channel, corrections of LST for atmospheric effects and for effects related to the emissivity of real surfaces cannot be made directly from image data; external data must be involved. The method of LST calculation applied in this study is described below and the flowchart in Fig. 2 summarizes the basic steps of this process.

For the first step, the unitless digital numbers (DN) of the thermal band were converted into top-of-atmosphere radiance (L_{TOA}) in Watts per square meter per steradian per micrometer:

$$L_{TOA} = \frac{L_{\max} - L_{\min}}{QCA\,L_{\max} - QCA\,L_{\min}}(DN - QCA\,L_{\min}) + L_{\min}, \quad (1)$$

where $\mathrm{QCAL}_{\min}$ (0) and $\mathrm{QCAL}_{\max}$ (255) are the lowest and the highest values of the range of rescaled radiance in DN.

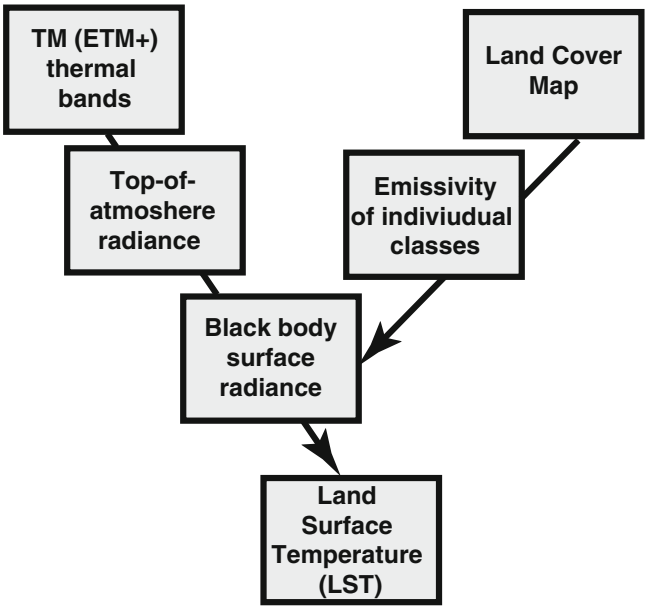

Fig. 2 Flowchart summarizing basic steps of LST derivation from single-band thermal infrared imagery. See text for further explanation

Further L_{min} (0) and L_{max} (17.04 Wm^{-2} sr^{-1} μm^{-1}) are the lowest and the highest radiances corresponding to $QCAL_{min}$ and $QCAL_{max}$.

In the second step, the top-of-atmosphere radiance was transferred to surface leaving radiance by removing atmospheric effects, employing the Atmospheric Correction Parameter Calculator developed by Barsi et al. (2005). This tool uses the MODTRAN radiative transfer model to calculate the three parameters that are necessary for atmospheric correction: upwelling radiance (L_u), downwelling radiance (L_d), and transmission coefficient (τ). Thus, the radiance of a black body surface with kinetic temperature T (L_T) can be expressed as:

$$L_T = \frac{L_{TOA} - L_u - \tau(1-\varepsilon)L_d}{\tau\varepsilon} \quad (2)$$

In which ε represents the emissivity of a real surface. A land-cover map was created to make the emissivity correction. This was done by supervised classification of satellite imagery using visible and short infrared bands, with a typical emissivity coefficient assigned to each land-cover category (Snyder et al. 1998). In the final step, radiances L_T were recalculated to surface temperatures by applying Planck function (Chander and Markham 2003):

$$LST = \frac{K_2}{\ln\left(1 + \frac{K_1}{L_T}\right)}, \quad (3)$$

where LST is land surface temperature in Kelvin (K). K_1 and K_2 are calibration constants that reach the following values for ETM+ imagery: K_1=666.09 W m^{-2} sr^{-1} and K_2=1,282.71 K. Corresponding values for TM are: K_1=607.76 Wm^{-2} sr^{-1} and K_2= 1,260.56 K (Chander et al. 2009). According to Barsi et al. (2005), uncertainties in LST related to the above method of atmospheric correction should be less than 2 K and a similar approach was used, e.g., by Yuan and Bauer (2007) for Minnesota. Calculated LST values were finally scaled from Kelvin to degrees Celsius.

Normalized difference vegetation index (NDVI) was calculated from satellite imagery in the following way:

$$NDVI = \frac{IR - VIS}{IR + VIS} \quad (4)$$

In which IR represents spectral reflectance in short infrared (band 4 in terms of Landsat data) while VIS stands for spectral reflectance in the visible part of the electromagnetic spectrum (band 3). NDVI is unitless and its values range theoretically from −1 for surfaces with no vegetation to 1 for parts with dense vegetation cover. Thus NDVI can be used to map the abundance and vigor of vegetation and this measure is frequently used in urban remote sensing as well, as a factor influencing LST variability and surface UHI structure (Dousset and Gourmelon 2003; Yuan and Bauer 2007; Weng 2009).

The GIS database of polygon shapefiles for building footprints was used to calculate density of buildings (DENS). The study area was divided into a regular 300×300-m grid and for each cell the DENS value was calculated as a percentage of building area located in the individual grid. Whereas NDVI quantifies the occurrence of natural surfaces within each grid cell, DENS value describes the degree of anthropogenic transformation and represents the amount of impervious surfaces, which is usually related to higher LST and significantly contributes to surface UHI formation. The size of the grid (300 m square) was chosen on the basis of a literature review and with reference to similar studies. According to Oke (2006), the circle of influence of environmental parameters, such as building density, upon temperature measurements may have a radius of about 0.5 km, depending on local conditions. Unger (2004) characterized relationships between surface geometry and the urban heat island in Szeged (Hungary) with a 500-m grid and Hart and Sailor (2008) quantified the influence of land-use and surface characteristics on urban temperatures in Portland (USA) using 300-m grid. Sampling at a 300-m grid size was selected for this study in view of the relatively high

heterogeneity of the environment, especially in the suburbs (see Fig. 1b).

4 Results

4.1 LST variability related to land-cover types

Analyzed Landsat thermal infrared images provided spatially consistent and detailed information on LST variation in the study area. This information is valid for the two dates of image acquisition, but some common features appear in both cases and allow us to generalize our findings to some extent.

In spite of the similar weather type and circulation patterns occurring on both dates, air temperatures were higher on 15 June 2006 compared to 24 May 2001. This difference is even more clearly expressed in satellite-derived LST values. Mean LST for the entire study area for the above dates reaches 19.1 and 31.7 °C, respectively. However, the LSTs show similar spatial distribution on both dates, especially in the built-up areas. The surface temperatures of built-up areas were clearly higher compared to the rural landscape in the immediate surroundings (Fig. 3). Very high LSTs are apparent not only in built-up areas, but also partly on arable land. Further, several cold spots may also be distinguished near the city center, related to city parks and recreational areas. Because a distinct spatial structure of LSTs with lower/higher values can be found within the built-up areas, analysis of LST variability was performed for the six land-cover classes introduced in Section 2.

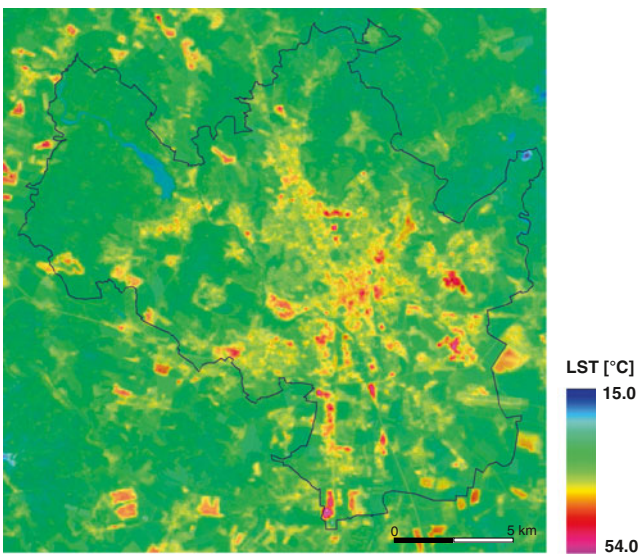

Fig. 3 Spatial variability of LST values within the Brno region; LST derived from Landsat thermal imagery acquired on June 24, 2006

For this purpose, a map of land-cover classes was superimposed onto the LST map to estimate the contribution of individual classes to LST variability and surface UHI intensity. The results of this analysis are presented in Fig. 4.

The LST values summarized in the form of box plots on Fig. 4 are especially representative of the land cover categories that take up a high percentage of the study area. Since the categories of city parks and water bodies each represent only about 1 % of the area, LSTs derived for these two classes can be noisy. In both the cases analyzed, the warmest category is that of industrial, commercial and transport areas. Great variability and the occurrence of the highest LSTs is also typical of this category. Residential areas are the second warmest category on both dates. Agricultural areas and forests, as representatives of rural landscapes, are significantly cooler. Arable land exhibits high variability, with very high maximum surface temperatures comparable to those of industrial areas, especially for the 2006 image. Very high LSTs occurring in agricultural areas are characteristic of fields with low percentages of vegetation cover, which usually warm up quite quickly during the morning hours. Sparse vegetation also means drier conditions and the low latent heat transfer that usually cools down areas with higher percentages of vegetation. Together with the area of the water reservoir, the forests fell into the coolest category. The low LSTs of forests are partly related to the fact that this category occupies the highest altitudes within the study area.

Surface UHI intensity was estimated as the difference between typical urban and rural areas. Of the above six land-cover classes, residential and industrial areas may be put together to represent the urban environment with typical artificial surfaces, while arable land and forest classes represent the rural areas. City parks and bodies of water were not included in this urban–rural comparison because both categories take up only a small percentage of the study area. Moreover, the category of city parks and recreational areas is heterogeneous in terms of land cover. Thus, a simple difference between mean LST of urban and rural categories may be considered as a measure of the overall surface UHI intensity in the Brno area and is presented in the form of a box plot in Fig. 5.

It follows from Fig. 5 that LSTs in the urban and rural areas of the Brno region differ significantly. Surface UHI intensity reaches 4.2 °C for 2001 and 6.7 °C for 2006, while LST variability is similar in both environments. The ranges of LST values (max–min) for urban and rural areas are not consistent for both dates. However, these absolute extremes of LST may be strongly influenced by several factors, such

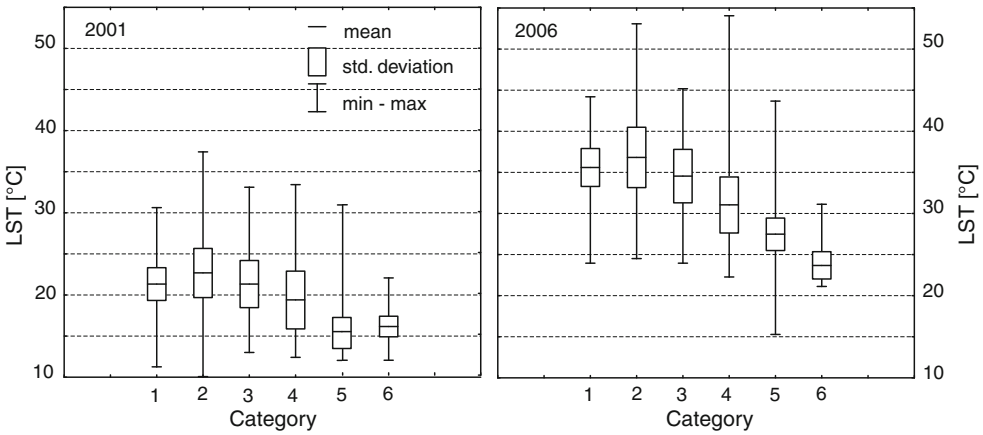

Fig. 4 *Box plots* of LST values for individual land cover classes

as radiometric errors in thermal imagery, atmospheric effects, and more.

The contribution of individual land-cover classes to surface UHI formation and its intensity on both dates is estimated in Table 1. For a better comparison of the two cases analyzed, LST values for individual categories were expressed as deviation from the mean LST value calculated over the whole study area. This differencing provides a better means of comparison between the 2001 and 2006 LST maps. Moreover, expression of LST as anomaly can partly eliminate potential bias arising out of atmospheric effects since these effects may be considered constant over the relatively small study area.

From Table 1, it follows that the LSTs of industrial areas can be 3–5 °C warmer compared to the mean surface temperature of the whole study region. Thus, industrial areas contribute the most to higher LSTs in the urban environment and they also heighten surface UHI intensity. The contribution of residential areas is slightly lower. The latter category usually contains some percentage of vegetation in open spaces as well as impervious built-up areas. While LSTs for arable land and grassland do not significantly deviate from the mean values, the forests are clearly cooler.

A closer look at LST variability and surface UHI structure in the city center is presented in Fig. 6. In this figure, areas with LST higher than the mean+2 SD are outlined in black and these areas represent hot spots within the built-up area of Brno. The accompanying aerial photographs show that these hot spots with significantly higher LSTs fall into the industrial, transport, and commercial category. The most extensive areas of high surface temperatures include large factories, industrial complexes, the large railway marshaling yard, and shopping centers/malls. Most of these apparent hot spots are concentrated southeast of the city center.

4.2 Other factors affecting LST variability

The above analysis shows that land-cover categories demonstrate typical LST variability and that such categories facilitated description of surface UHI intensity in the study region. Even though the land-cover classes reflect the degree of anthropogenic transformation of the area, urban/rural character can be described more precisely in terms of surface parameters that are continuous in space. Various such surface parameters are frequently used in urban climatology (Weng et al. 2004; Yuan and Bauer 2007; Hart and Sailor 2008; Hu and Jia 2010).

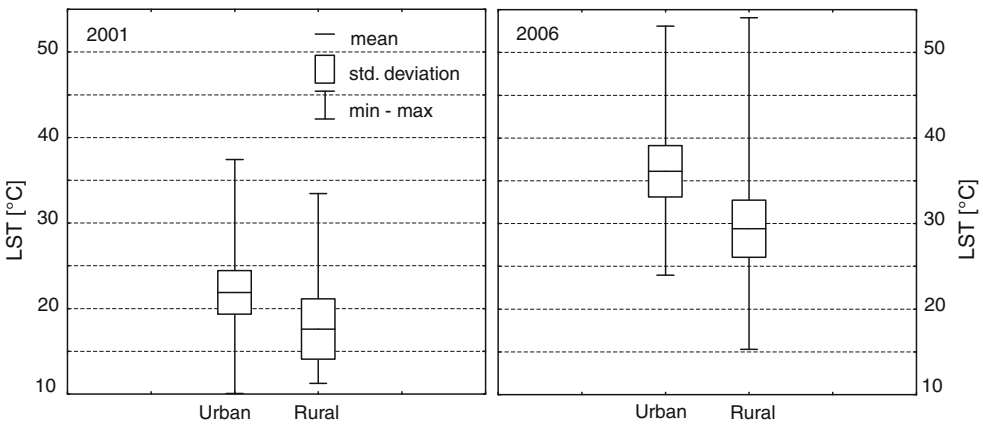

Fig. 5 Intensity of surface UHI in Brno region defined as the difference between urban and rural areas for two analyzed scenes

Table 1 Mean LSTs for individual land cover categories expressed as anomalies with respect to the mean LST over the study area

Category	LST anomaly 2001 (°C)	LST anomaly 2006 (°C)
Residential areas	2.2	3.9
Industry and transport areas	3.5	5.1
City parks and recreational areas	2.2	2.8
Arable land and grasslands	0.3	−0.7
Forests and orchards	−3.7	−4.2
Water bodies	−3.2	−8.0

Positive values indicate above-average LSTs and vice versa

In this study, vegetation index (NDVI) and density of buildings (DENS) were used as predictors of LST variability within the study area (see Section 3). Both dependent (LST) and independent (NDVI, DENS) variables were re-scaled to the same resolution (a 300× 300-m grid), while DENS values were further transformed using Box–Cox transformation to satisfy the normality assumption. As an example, Fig. 7 summarizes simple regression models between LST and respective explaining variables for the 15 June 2006 case. LST shows significant negative correlations with NDVI and explained variance reaches 56 and 67 % for the 2 years analyzed. This means that the occurrence of vegetation cover can significantly reduce LST values in an urban environment. Transformed DENS values correlate positively with LST. Thus higher density of built-up areas corresponds to higher surface temperatures. Even if the explained variance is lower compared to NDVI, correlations between DENS and LST are statistically significant ($p<0.05$) for both dates. The density of buildings explains 40 % of LST variability calculated from the 2001 Landsat thermal image; this is 37 % for the 2006 image.

Fig. 6 Spatial distribution of LST in the center of Brno. *Black lines* mark surround with LST higher than the mean+2 SD. *Individual numbers* indicate the positions of selected "hot spots" with character of land cover as presented on the accompanying aerial photographs

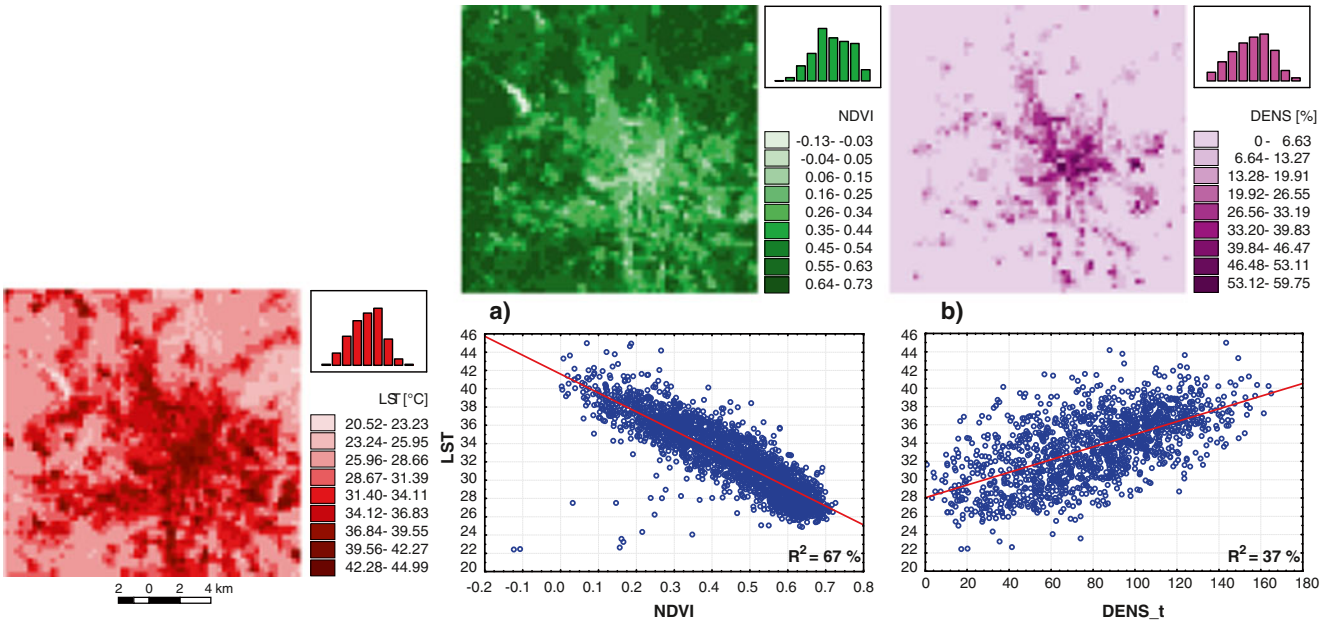

Fig. 7 Linear regression between LST and NDVI (**a**) and between LST and DENS (**b**) in the Brno region (LST and NDVI data is from June 15, 2006). DENS_t values in scatter plot mark DENS values transformed using Box–Cox transformation and R^2 expresses explained variance

5 Discussion

While satellite-derived LSTs and surface UHI intensity have recently been analyzed for several large cities and for cities from various climatic zones, this study addresses LST spatial variability and surface UHI phenomenon using a medium-sized central European city with a varied environment as an example.

LSTs derived from high spatial resolution Landsat data show clear differences for individual land-cover categories. Industrial and commercial areas are in the warmest category and some of these areas form distinct hot spots in the Brno region. Residential areas are slightly cooler and LSTs do not reach such extreme values as in industrial areas. This is in agreement with similar comparable studies and these two types, which comprise the majority of built-up areas, significantly contribute to surface UHI intensity in the Brno region. While the forest areas demonstrate a clear cooling effect, some agricultural fields exhibit high LSTs, comparable with built-up areas. This occurs mainly with patches of arable land that have a low percentage of vegetation cover. The two examples of thermal infrared imagery analyzed indicate that surface UHI intensity in the Brno region can reach 4–7 °C.

As for the amount of LST-explained variance, from the analysis it follows that the amount of vegetation cover represented by NDVI is of higher importance than the degree of urbanization represented by density of buildings. This is in agreement with the conclusions of, e.g., Dousset and Gourmelon (2003) for Paris. Gallo and Owen (1999) also found that vegetation cover accounts for 40 % of the urban–rural temperature difference. Our results, ranging from 56 to 67 % are in agreement with those of Hu and Jia (2010), who found that NDVI explains 61 % of LST variability. However, the surface characteristics most important to LST variability, and subsequently to surface UHI intensity, can be different, depending upon city morphology, location, and climatic zone (Hart and Sailor 2008). Thus, for instance, Yuan and Bauer (2007) concluded that the relation between LST and percentage of impervious surface is more significant while NDVI importance is less strong and the role of vegetation varies with the seasons. The satellite thermal images available for the current study for the Brno region did not permit study of the seasonal aspect. Moreover, the density of buildings used in this study tends to represent the mass of buildings and involves only a part of the impervious surfaces. As well as the amount of buildings, other subcategories may also be considered in the makeup of the surface parameter representing impervious or more generally anthropogenic surfaces. For instance, we demonstrated that a parameter measuring the total length of the streets and communications in each 300×300-m grid cell explained almost 20 % of the LST variability in Brno area (analysis not shown here). Both the density of buildings used in this study and the total length of streets can be relatively simply calculated from the GIS database and our results demonstrate that they can be used as an alternative to the category of impervious surfaces that is usually derived

from satellite imagery using image processing methods such as the spectral mixture model (Weng 2009) or the vegetation–impervious surface–soil model (Ridd 1995).

Future activity will focus on LST analysis from ASTER data, because this system provides five thermal bands and permits the derivation of both LST and band emissivities directly from image data. Finally, thermal imagery for a higher number of days could provide more reliable and more robust results.

6 Conclusions

The study area of Brno is not characterized by the dynamic development and rapid land-cover and land-use changes found, for example, in the cities of eastern Asia. Even though Brno's changes are gradual in comparison, one of the most pronounced long-term land-use changes in the sub-urban zones of the Czech Republic relates to an areal expansion of built-up areas at the expense of natural surfaces (Bičík and Jeleček 2009). Moreover, according to Brázdil et al. (2009), there has been a significant increasing trend in air temperature since 1960s, while precipitation quantities have tended towards a decrease in Brno. Thus such gradual processes may act in synergy to magnify the possible risk of the negative impacts of adverse weather and climate phenomena, such as longer and more intense heat waves, and periods of drought or low humidity. Based on two highly-resolved thermal infrared images from the summer season and the GIS database, the present study provides, above all: (a) an assessment of surface UHI intensity; (b) a contribution of land-cover categories to surface UHI formation; (c) a spatial structure for urban thermal patterns with delimitation of hot spots in a built-up area; and (d) quantification of the role of vegetation cover and density of buildings in variability of surface temperatures. These findings may be valuable to urban and regional planning and to urban ecology.

Acknowledgements This study was prepared within the project GA205/09/1297 "Multilevel analysis of the urban and suburban climate taking medium-sized towns as an example" granted by Czech Science Foundation. Tony Long (Svinošice, Czech Republic) is acknowledged for English style corrections.

References

Arnfield AJ (2003) Two decades of urban climate research: a review of turbulence, exchanges of energy and water, and the urban heat island. Int J Climatol 23:1–26

Barsi JA, Schott JR, Palluconi FD, Hook SJ (2005) Validation of a web-based atmospheric correction tool for single thermal band instruments. Proc SPIE 5882:136–142

Bičík I, Jeleček L (2009) Land use and landscape changes in Czechia during the period of transformation 1990–2007. Geografie 4:263–281

Brázdil R, Chromá K, Dobrovolný P, Tolasz R (2009) Climate fluctuations in the Czech Republic during the period 1961–2005. Int J Climatol 2:223–242

Chander G, Markham BL (2003) Revised Landsat-5 TM radiometric calibration procedures and postcalibration dynamic ranges. IEEE T Geosci Remote 41:2674–2677

Chander G, Markham BL, Helder DL (2009) Summary of current radiometric calibration coefficients for Landsat MSS, TM, ETM +, and EO-ALI sensors. Rem Sens Environ 113:893–903

Cheval S, Dumitrescu A (2009) The July urban heat island of Bucharest as derived from modis images. Theor Appl Climatol 96:145–153

Dash P, Göttsche FM, Olesen FS, Fischer H (2002) Land surface temperature and emissivity estimation from passive sensor data: theory and practice—current trends. Int J Rem Sens 13:2563–2594

Dousset B, Gourmelon F (2003) Satellite multi-sensor data analysis of urban surface temperatures and landcover. ISPRS J Photogramm 58:43–54

Dousset B, Gourmelon F, Laaidi K, Zeghnoun A, Giraudet E, Bretin P, Mauri E, Vandentorren S (2011) Satellite monitoring of summer heat waves in the Paris metropolitan area. Int J Climatol 31:313–323

Gallo KP, Owen TW (1999) Satellite-based adjustments for the urban heat island temperature bias. J Appl Meteor 38:806–813

Grimmond S (2006) Progress in measuring and observing the urban atmosphere. Theor Appl Climatol 84:3–22

Hart MA, Sailor DJ (2008) Quantifying the influence of land-use and surface characteristics on spatial variability in the urban heat island. Theor Appl Climatol 95:397–406

Hu Y, Jia G (2010) Influence of land use change on urban heat island derived from multi-sensor data. Int J Climatol 9:1382–1395

Kato S, Yasushi Y (2005) Analysis of urban heat island effect using ASTER and ETM+ Data: separation of anthropogenic heat discharge and natural heat radiation from sensible heat flux. Rem Sens Environ 99:44–54

Lambin E, Geist H (eds) (2006) Land-use and land-cover change. Local processes and global impacts. Springer, Berlin

Li F, Jackson TJ, Kustas WP, Schmugge TJ, French AN, Cosh MH, Bindlish R (2004) Deriving land surface temperature from Landsat 5 and 7 during SMEX02/SMACEX. Rem Sens Environ 92:521–534

Nichol JE (1998) Visualization of urban surface temperatures derived from satellite images. Int J Rem Sens 9:1639–1649

Oke TR (1997) Urban climates and global environmental change. In: Thompson RD, Perry A (eds) Applied climatology. Routledge, London, pp 273–287

Oke TR (2006) Initial guidance to obtain representative meteorological observations at urban sites. IOM Report No. 81, WMO/TD. No. 1250. World Meteorological Organization, Geneva

Pongracz R, Bartholy J, Dezso Z (2006) Remotely sensed thermal information applied to urban climate analysis. Adv Space Res 37:2191–2196

Qin Z, Karnieli A, Berliner P (2001) A mono-window algorithm for retrieving land surface temperature from Landsat TM data and its application to Israel–Egypt border region. Int J Rem Sens 18:3719–3746

Ridd MK (1995) Exploring a V-I-S (vegetation–impervious surface–soil) model for urban ecosystem analysis through

remote sensing: comparative anatomy for cities. Int J Rem Sens 16:2165–2185
Snyder WC, Wan Z, Zhang Y, Feng Y (1998) Classification-based emissivity for land surface temperature measurement from space. Int J Rem Sens 19:2753–2774
Sobrino JA, Jiménez-Muñoz JC, Paolini L (2004) Land surface temperature retrieval from LANDSAT TM 5. Rem Sens Environ 90:434–440
Stathopoulou M, Cartalis C (2007) Daytime urban heat islands from Landsat ETM+ and Corine land cover data: an application to major cities in Greece. Sol Energy 81:358–368
Stewart ID (2011) A systematic review and scientific critique of methodology in modern urban heat island literature. Int J Climatol 2:200–217
Tan KC, Lim HS, MatJafri MZ, Abdullah K (2010) Land surface temperature retrieval by using ATCOR3_T and normalized difference vegetation index methods in Penang Island. Am J Appl Sci 5:717–723
Tomlinson CJ, Chapman L, Thornes JE, Baker CJ (2010) Derivation of Birmingham's summer surface urban heat island from MODIS satellite images. Int J Climatol. doi:10.1002/joc.2261
Unger J (2004) Intra-urban relationship between surface geometry and urban heat island: review and new approach. Clim Res 27:253–264
Voogt JA, Oke TR (2003) Thermal remote sensing of urban climates. Rem Sens Environ 86:370–384
Weng Q (2009) Thermal infrared remote sensing for urban climate and environmental studies: methods, applications, and trends. ISPRS J Photogramm 64:335–344
Weng Q, Lu D, Schubring J (2004) Estimation of land surface temperature–vegetation abundance relationship for urban heat island studies. Rem Sens Environ 89:467–483
Yuan F, Bauer ME (2007) Comparison of impervious surface area and normalized difference vegetation index as indicators of surface urban heat island effects in Landsat imagery. Rem Sens Environ 106:375–386